# Characterization of the granular dynamics at the interface between a pipe and a granular flow in a rotating drum

François Rioual*, Paule Emmanuelle Eva Gbehe

*Research Unit FRISE, National Research Institute for Agriculture Food and the Environment, 1 rue Pierre Gilles De Gennes, 92160, Antony, France*

**Abstract**

A new mobile bed heat exchanger is presented in this work which is composed of a flowing granular material in a rotating drum and a cylindrical pipe with potential interest in different energy applications as cooling, heating or heat recovery processes. An optimal design of the device requires a characterisation of the phenomena involved at the interface between the granular flow and the pipe. The process is modelled by the discrete element method and a global classification of the flow patterns around the pipe is presented with respect to the three main control parameters of the problem: the Froude number, the diameter ratio and the relative filling height of the drum. The second part is devoted to the characterisation of the structure of the flow at the interface (velocity field, density field) in particular in a so-called *Biflow* regime where granular motion occurs above as well as below the pipe which is favorable to transfer by convection. A typical behavior at the interface with the pipe consists of a zone I with high velocities of particles at the top of the pipe, a second zone with quasistatic particles or low velocity particles at the front and at the bottom of the pipe and a last zone III of depletion of particles at the back of the pipe. The Froude number has a limited effect on the features of this structure on the first layer in the range of Froude numbers considered whereas the relative height is a more determinant parameter to control the relative magnitude of velocities in zone I and zone II as well as the extent of the depletion zone. This first hydrodynamical characterisation can shed light on the dynamical regimes with improved transfer between the particles and

*Corresponding author

*Email address:* francois.rioual@inrae.fr (François Rioual )

the pipe boundary.

*Keywords:* Granular flow, Transfer, Heat exchange, Mobile bed, Boundary condition

## 1. Introduction

Mobile bed heat exchangers (MBHE) are indirect exchangers using a granular material flowing by gravity along a surface of transfer (tube, plate). They received an increasing interest these last year as a low cost and efficient solution for heat transfer in solar power plants [1, 2] or as a heat recovery process for an alternative electric production [3]. The concern of the scientific community for such systems increased therefore recently in a significative way [2, 4] as the proper characterisation of the coupling between heat transfers [6] and the complex rheological properties of dense granular flows [5] still require important efforts. Thermal transfers in granular flows can be essentially examined through modelling approaches as the discrete element method that can give access to relatively reliable thermal field in the bulk at the grain scale [7, 8, 9, 10, 11, 12] despite recent warnings [13] whereas experimental approaches can give access only to measurements of effective transfer coefficients [14, 15] at the macroscopic scale or temperature fields on a given external surface with infrared thermography as proposed recently [16].

Concerning the characterisation of heat transfers between a simple gravity driven granular flow and a duct, recent modelling works [4] show the major role played by the motion of the grains along the surface of exchange. Energy efficiency appears limited on one hand by the apparition of a zone of accumulation of quasistatic particles at the front of the pipe with respect to the flow direction: In fact thermal gradients decrease with time in the static zone of particles and are much smaller than those imposed by the contact of new mobile particles of the flow. Such cone shaped stagnant area have also been studied experimentally [17, 18] and are very relevant for the design of MBHE. The modelling approach [4] shows also that a higher velocity of the particles is associated to an increased transfer for the same reason of more frequent renewal of the neighboorhood of contact. On the other hand, the apparition of a zone of depletion of particles at the back of the pipe cancel obviously the thermal transfers along this portion of pipe. The same authors evoke also a mixing zone between different layer of particles on the exposed part of the pipe created by the curvy outline: this is also favourable to the transfer by allowing a possible access at the boundary of the some remote

particles. However, these interesting works show that the phenomena of jamming, depletion and mixing are interdependant and play sometimes contrary roles with respect to the total transfer. The work of Guo et al. [4] illustrates in particular the strong coupling between granular mechanics around the pipe and transfer which motivates generally a careful analysis of the flow [18].

We would like in this work to analyse the evolution of the hydrodynamic characteristics of a mobile granular bed in contact with a pipe in an original MBHE device where the granular flow is generated continuously by the surface flow of a moving granular material partially filling a rotating drum. Our practical motivation is to identify the parametric conditions for an improved transfer between the moving granular bed and the pipe.

The first section of this article is devoted to the presentation of the new device, its potential benefits and the computational methodology to model the flow. The second section presents the results of the study: First, a global classification of the different flow patterns that appear around the pipe is established according to the main control parameters of the problem: The Froude number $Fr$, the diameter ratio $\frac{R_d}{R_p}$ and the effective height of the packing $h_0 = \beta r_p$ where $\beta$ is a scale parameter. These results can be summarised in a bed behavior diagram. Second, the structuration of the flow around the pipe is quantified through the calculation of the average velocity and average density field of particles on the first layer at the contact with the pipe with respect to the control parameters. We discuss at last some implications for the transfer at the light of these previous results.

## 2. Materials and methods

### *2.1. Presentation of the device*

The device consists in a horizontal rotating drum (radius $R_d$, length $P$) and a fixed pipe (radius $R_p$) located along the rotation axis of the drum. The drum is filled with a granular material (particle radius $r$) at a certain height $h_0$ measured from the centre of drum as a fraction $\beta$ of the pipe radius $R_p$. The rotation of the drum at a velocity $\omega$ will generate a granular flow at the surface that we want to study in order to maximize the heat transfer between the granular material and the pipe. Figure 1 shows the principle of the new mobile bed heat exchanger and the dimensions of the device are detailled on Table 1.

| Dimensions | Value |
|---|---|
| **Drum radius** $R_d$ | 0.2 m |
| **Drum length** $P$ | $40r = 0.16$ m |
| **Pipe radius** $R_p$ | $3/10R_d$; $R_d/5$; $R_d/10$; $R_d/15$ |
| **Particle radius** $r$ | 0.004m $\pm 10\%$ |
| **Rotation velocity** $\omega$ | 10 rpm ; 20 rpm ; 30 rpm ; 40 rpm |

Table 1: Numerical values of the dimensions in the device

The configuration of rotating drum is widely used in the chemical engineering of divided matter, in numerous industries for mixing, drying, grinding, coating, granulation, chemical and biochemical reaction and so on from large particles of minerals to food powders and pharmaceutical ingredients. Heat transfer plays a significant role in many of these processes in which granular materials are generally heated indirectly through the rotating wall [20]. By increasing the angular velocity of the drum,the surface flow goes from of a regime of intermittent avalanche then to a continuous regime of avalanches and to a flow regime of curved surface involving a thicker active layer [21]. This last cascading regime although poorly studied provides suitable operational conditions for industrial mills and granulators for instance [22]. In particular, the active flowing layer thickness is an important quantity for these processes. Our exchanger will be mostly exploring the cascading regime because of the expected thicker width of the active layer where it allows also a continuous recirculation of the flow along the pipe. Compared to classical gravity driven mobile bed heat exchangers, the continuous motion of recirculation of the particles along the pipe, created by the rotating drum, allows to control the amount of heat transferred towards a reduction of the temperature differential between the pipe and the particles. Simplicity of installation and energy savings may also be more reachable compared to indirect rotary coolers for instance because a simple pipe embedded in the granular flow along the drum axis is necessary and there is no need to dive the entire drum in a thermostated bath. At last, the regular recirculation of the granular material around the pipe by rotation may also create a possible mixing effect of the particles in the drum after several rotations eventually through transient granular vortices [19] potentially relevant to transfers [23]. However these favorable conditions have to be analysed and clarified in more details.

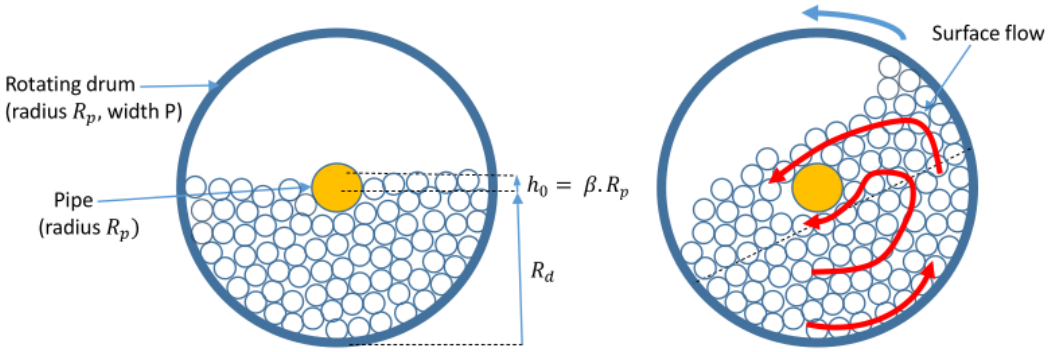


Fig. 1: Principle of the mobile bed heat exchanger in a rotating drum - front view (left) and sketch of the flow in the *Biflow* regime (right)

### *2.2. Computational methodology*

We chose to model the granular flow in the new device and in particular the mechanical properties of the flow in contact with the pipe with the discrete element method. The discrete element method is a successful technique developped by Cundall and Strack in 1970 in order to model the dynamics of granular matter in different contexts [24]. Its principle consists in modelling each particle as a discrete unit where its dynamic under external forces (frictional collisional contacts with neighbouring particles and boundaries) is resolved using Newton's second law of mechanics. The present model has been implemented on the Open-source software Yade-dem [25]. In this frame, the choice of the constitutive law for the model of contact is crucial to be able to describe the physics at the particle scale. We chose in this work a visco-elastic contact law in the normal and tangential direction with Coulomb friction in the tangential direction. This law is simple enough and able to describe energy dissipation for dense granular flows [26]. Input mechanical parameters for using this law are: Young modulus, Poisson coefficient and normal and tangential restitution coefficients. The stiffness coefficient as the damping constants are deduced from the value of the normal coefficient of restitution that can be determined experimentally. We used as reference materials for the particles and the boundaries (inner cylinder, drum walls) respectively glass and plexiglass. It is important to precise that the values of the Young moduli chosen do not correspond to the real values of the materials. Indeed a practical way to decrease the computational time is to choose smaller values for the Young moduli (softer beads) so that the time step of the simulation is longer. Nevertheless we checked that the interpenetration between particles remains weak

(interpenetration less than 1% of the particle size). The numerical values of material properties are presented on Table 2. Parameters of the model in DEM are deduced from the material properties of each participant of the interaction (wall or particle): for the stiffness as the stiffness of two springs in serial configuration or for other parameters by taking the average of material parameters [25].

| **Material property** | **Value** |
|---|---|
| **Wall density** | 1190 kg/m $^3$ |
| **Wall Poisson ratio** | 0.37 |
| **Wall Young modulus** | $10^5$ Pa |
| **Particle density** | 2500 kg/m $^3$ |
| **Particle Poisson ratio** | 0.3 |
| **Particle Young modulus** | $10^6$ Pa |
| **Wall normal coefficient of restitution** | 0.920 |
| **Particle normal coefficient of restitution** | $15/16$ |
| **Wall tangential coefficient of restitution** | 1 |
| **Particle tangential coefficient of restitution** | 1 |
| **Wall coefficient of friction** | 0.8 |
| **Particle coefficient of friction** | 0.7 |

Table 2: Numerical values of the material properties

In a first step, flow patterns have been qualitatively analysed through a representation of the velocity field that are obtained from Yade-dem tools (yade module yade.post2d) for the projection of 3D points to 2D with an autoscaling algorithm based on average vector length and number of vectors [25]. In order to characterize the hydrodynamic behavior at the contact with the pipe boundary, we calculated in a second step through different python scripts the mean density field (particle volume fraction) and velocity field discretized in bins in a cylindrical ring of interest of one particle width around the pipe (20 bins constituting the mesh corresponding to an angular step of $\frac{\pi}{10}$). We performed a further averaging

of these physical quantities over one drum rotation and over different rotations in order to smooth small scale fluctuations of particle dynamics. The calculation of the effective packing fraction (density) can be delicate because of the complex detection of portions of beads at the boundaries of one bin. We used a voxel algorithm to treat this issue. This calculation method consists in dividing the whole volume into a dense grid of voxels (at given resolution), and count the voxels that fall inside any of the spheres. This method allows one to calculate porosity in any given sub-volume of a whole sample and is properly excluding a part of a sphere that does not fall inside a specified volume [25].

### *2.3. Dimensional analysis*

Dimensional analysis garantees that system properties expressed as non dimensional physical quantities depend only on non dimensional combinations of the physical parameters of the problem which limit advantageously the extent of the parametric study. Non dimensional parameters of the problem can be expressed as geometrical parameters: $R_d/r$; $R_d/R_p$ ; $P/r$ ; the height of the pile $\beta = h_0/R_p$ ; dynamical parameter as the Froude Number $R_d\omega^2/g$ as well as the mechanical parameters (Poisson, restitution and friction coefficients) and the stiffness number that measures the degree of deformation on a particle [27]. The present study is limited to the influence of three main parameters:

- Froude number
  The Froude number is the classical parameter used to classify flow regimes in simple rotating drums. it measures the relative importance of centrifugal forcing to gravity. The values of the Froude number are such that $2.24 * 10^{-2} < Fr < 3.57 * 10^{-1}$ corresponding to rotation velocities $\omega$ (Table 1). This range of values corresponds to the cascading regime and the beginning of cataracting regime in simple rotating drums [21].

- Relative height $\beta$
  $\beta$ is a scale parameter which quantifies the filling height $h_0$ of the packing obtained by $h_0 = \beta R_p$. The height of the packing scaled by the radius of the pipe is supposed to be determinant to control the flow in this problem. A range of values $-1 < \beta < 2$ has been chosen in this work.

- Ratio of the radius of the pipe to the radius of drum
  The ratio $\frac{R_d}{R_p}$ is also crucial for the determination of the influence of the size of the inner pipe on the flow. Following values $10/3; 5(C1); 10(C2); 15(C3)$ have been considered in this work.

## 3. Results and discussions

### *3.1. Bed behavior typology*

In order to get a qualitative overview of the different flow patterns around the pipe, we represented for each configuration the velocity field of the granular flow around the pipe. We observed a similar pattern for the different layer depths considered in the flow. For a global overview of the flow, we chose to represent the velocity field including all the particles in the drum on the same graph. In the range of parameters considered, we checked furthermore the global stationarity of the flow field in each configuration by observation of the different patterns at different times on one round. We represent in Appendix A a summary of the different flow patterns in the parameter space $(Fr, \beta, \frac{R_d}{R_p})$.

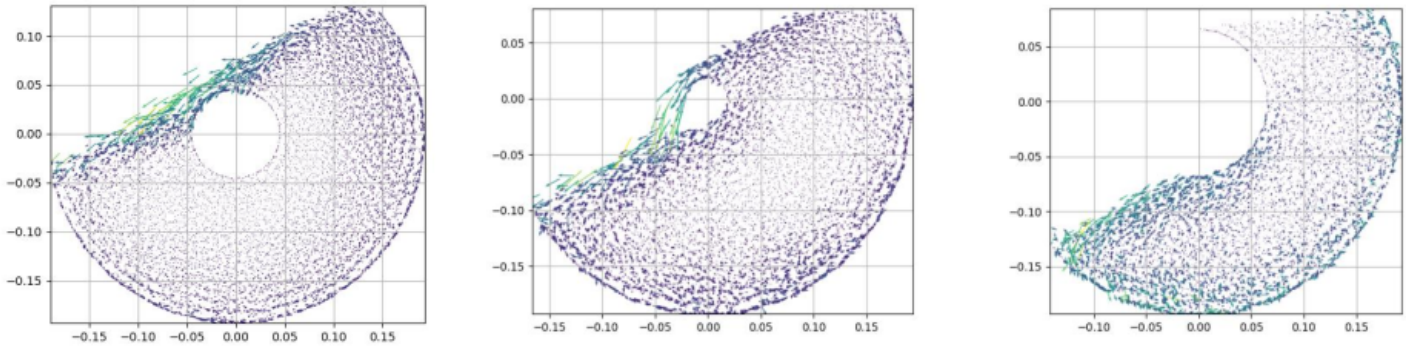

Fig. 2: Illustration of three main patterns observed: *Monoflow-up*(left) - *Biflow* (middle) - *Monoflow-down* (right)

The observation of the different configurations shows three main patterns for the flow around the pipe with respect to the control parameters that we called respectively *Monoflow-up* ; *Monoflow-down* and *Biflow* (Figure 2).

- *Monoflow-up* (MU)

  In this regime we observe a flow around the pipe that is essentially localised on the upper part of the pipe. The flow can have a plane surface or being curvy.

- *Monoflow-down* (MD)

In this regime, the surface flow is localised on the lower part of the pipe. An important zone of depletion of particles is observed at the top and on the back side of the pipe.

- *Biflow* (BF)

  This regime is characterized by a notable flow on both sides of the pipe (top and bottom). This is a relevant regime for our concerns because convection at the surface is thus maximized which is favorable to transfers.

The initial height of the bed appears to be a determinant parameter of the flow around the pipe: As the pile recovers entirely the interior duct ($\beta > 1$), we observe a regime *Monoflow-up* without any zone of depletion.As the initial height of the packing decreases, the flow relocate partly below the pipe; we enter in the regime called *Biflow*. As the initial height decreases, the flowing layer on the upper part of the pipe becomes thinner till we reach a transition to the regime *Monoflow-down* with an important zone of depletion. We note also that central zone shrinks progressively as the granular band in motion at the edges of the drum enlarges slightly.

The Froude number has an influence on the shape of the surface of the flow specially visible in the regime *Monoflow-up*. As the Froude number increases, we observe the apparition of curvy shape of the surface. This is consistent with classical observations in rotating drums when the filling ratio is higher that 10% and the Froude number $10^{-3} < Fr < 10^{-1}$ and known as the cascading regime [21]. We observe also that for higher sizes of the pipe, the curved shape appears for a lower Froude number. As for the effect of height, there is in fact also the contribution of the deviation of particle trajectories by the curvy surface of the pipe. At last, we note an increase of the width of the flowing layers with the Froude number also more quantitative characterization would be necessary. In cascading granular flows, the active flowing layer on top of the granular bed is indeed fed by the upward motion of particles driven by the rotation [22]. This trend is in agreement with previous results on the active layer in rotating drums [28] and might be also an interesting feature for transfer optimisation. The relative size of the pipe plays also an important role in the transition between the different regimes. For higher sizes of the pipe, the *Biflow* regime appears for lower $\beta$. This is consistent with the simple fact that higher depths of the flow have to be involved for higher pipe sizes in order to mobilize the lower layer at the bottom of the pipe.

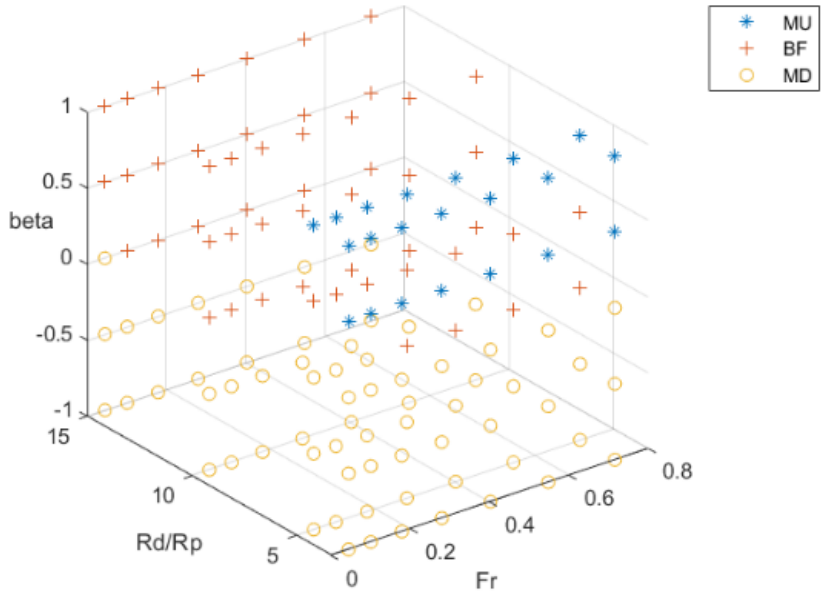


Fig. 3: Bed behavior diagram in the 3 parameters space (Froude number, relative height $\beta$, relative diameter ratio $R_d/R_p$)

A bed behavior diagram is represented on Figure 3 that summarizes our observations concerning the flow patterns.

### *3.2. Quantitative analysis - Biflow regime*

As observed previously, the *Biflow* regime identified is certainly the most relevant regime for our purpose as it will maximize convection at the contact with the surface of the pipe. First observations of the global flow structure in this regime show the presence of a zone of strong slow down and nearly jamming of particles on the side of the pipe facing the flow because of the geometrical obstruction of the pipe. Particles in this zone are submitted to strong fluctuations and their trajectory seem to result from the competition between two main flows (Figure 1, right):

- The gravity granular flow getting past the top of the pipe: It is mainly fed by the layers of beads the closest from the drum circonference. It is a free surface gravity flow at a higher velocity and only constrained by the lower layers and the curved outline of the pipe.

- The gravity granular flow going downwards below the pipe. It involves the layers of beads closer to the centre of the drum. It is a downward gravity flow

at a lower velocity starting from a lower height and constrained on both sides by the curved outline of the pipe and the friction with the upward bulk motion of particles driven by the rotation of the drum (passive layer).

In order to have a clearer view of the microscale properties of the *Biflow* regime at the interface with the pipe, we determined quantitatively the evolution of the mean velocity and packing fraction of particles for $0 < \beta < 1$ at the contact with the pipe boundary which is a relevant region for the thermal transfer through granular contacts.

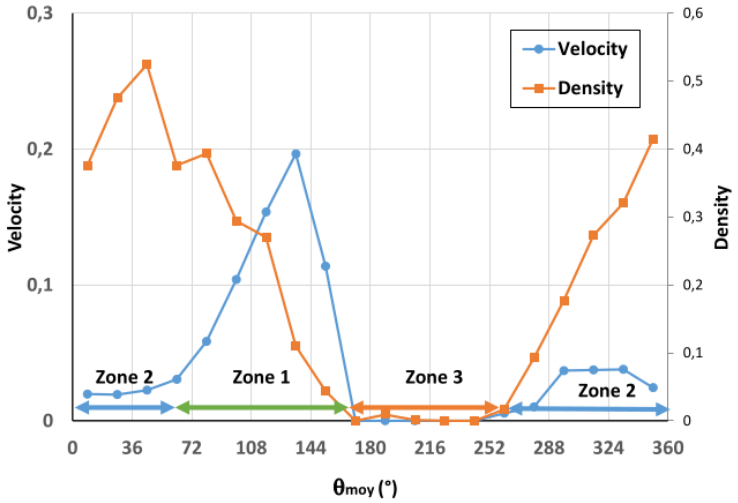


Fig. 4: Typical angular distribution of the velocity rescaled by the velocity of free fall from a height $R_d$, packing fraction as a function of the angular position $\theta_{\mathbf{moy}}$ around the pipe and definition of the three zones ($Fr = 0,05$, $\beta = 1$, $\frac{R_d}{R_p} = 10$ (c2))

We show on Figure 4 a typical evolution of these physical quantities around the pipe. We can define from the curve profiles three characteristic zone along the outline of the pipe:

- zone I

  The particles are localised at the top of the pipe. They have a high velocity and relatively low packing fraction. The evolution follows a roughly bell curve with respect to angular position with a maximum at around $130° - 150°$.

- zone II

The particles are localised on the bottom side of the pipe and on the side facing the flow. The velocities are low but we note that the particles are still moving in the *Biflow* regime contrary to free gravity MBHE [18]. A small maximum velocity is observed at an angular position around $290° - 330°$ below the pipe.

- zone III

  This is the depletion zone where no particles are in contact with the surface of the pipe.

We would like now to explore how these features evolve with the control parameters defined previously.

### *3.2.1. Influence of the Froude number*

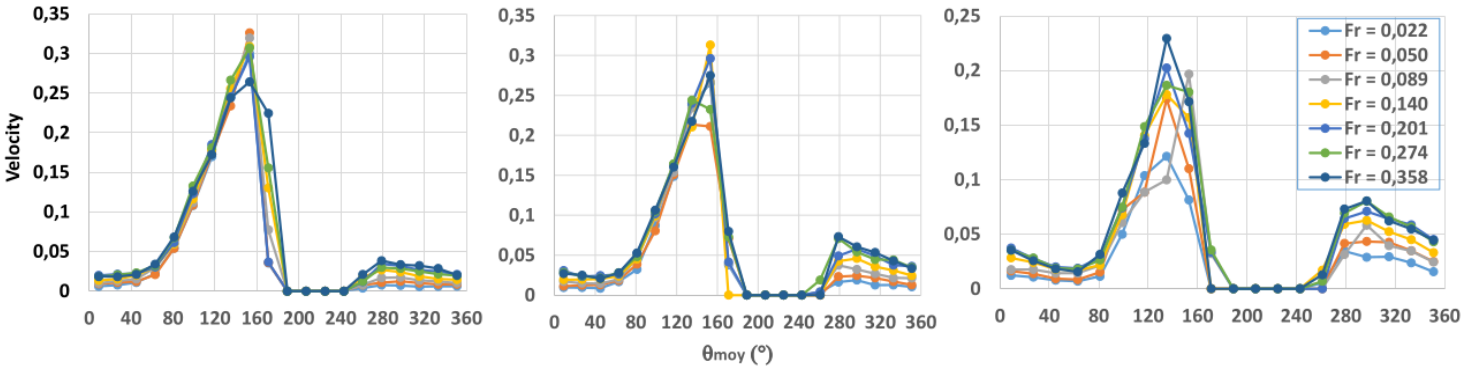


Fig. 5: Angular distribution of the velocity around the pipe for different Froude numbers and three different heights $\beta = 1$ (left) - $\beta = 0.5$ (middle) - $\beta = 0$ (right)

The evolution of the maximal velocity in zone I shows fluctuations and no clear correlation with the Froude number (Figure 5). Qualitative observations of the flow show that these particles are at contact from the jamming zone at the front of the pipe and favourable fluctuations in this zone can bring them with a low velocity at the top of the pipe under the drive of the high velocity upper layers of beads in a collisional regime.

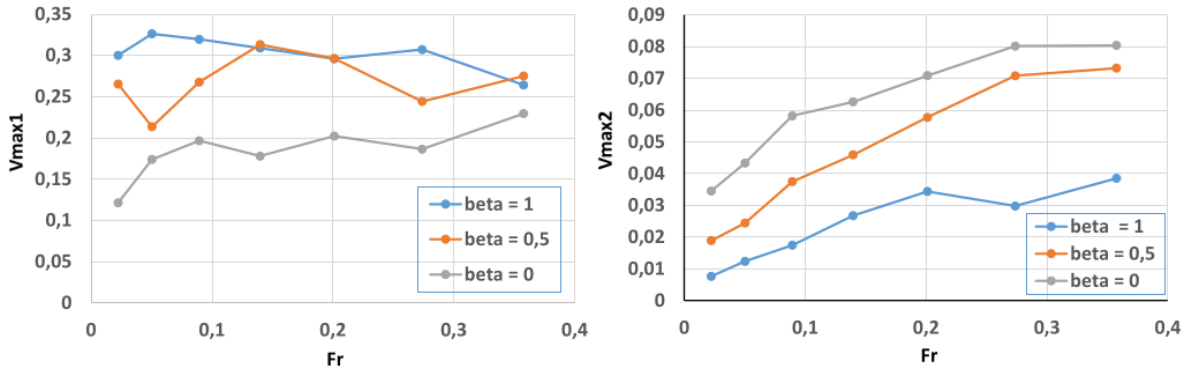


Fig. 6: Evolution of maximal velocity in zone I (left) and in zone II (right) as a function of the Froude number

On the contrary, the evolution of the the maximal velocity in zone II shows a regular increase with the Froude number (Figure 6) . We relate this fact to previous observations on cascading flows in simple drums that the width of the active layer increases with the Froude number in cascading flows implying higher velocities at a given depth. We note at last that the width of the different zones does not vary significatively with the Froude number in the limit of our discretisation procedure with a step size of discretisation of $\frac{\pi}{10}$.

### *3.2.2. Influence of the initial height of the packing*

This parameter appears to be determinant for the structure of the *Biflow* regime around the pipe.

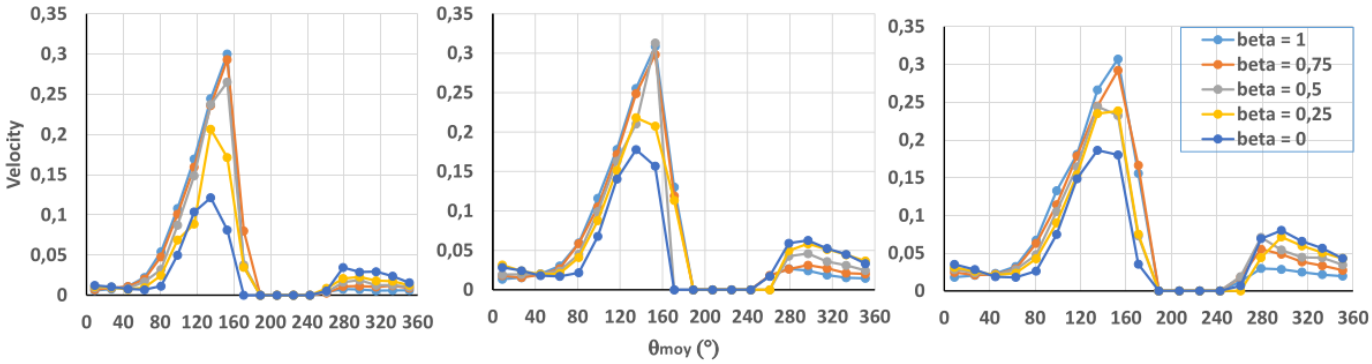


Fig. 7: Angular distribution of the velocity around the pipe for different initial heights $\beta$ at three different Froude numbers $Fr = 0.022$ (left); $Fr = 0.134$ (middle) ; $Fr = 0.274$ (right)

The typical evolution is shown on Figure 7. As the initial height decreases, the velocities in zone I decrease progressively as the velocities in zone II increase.

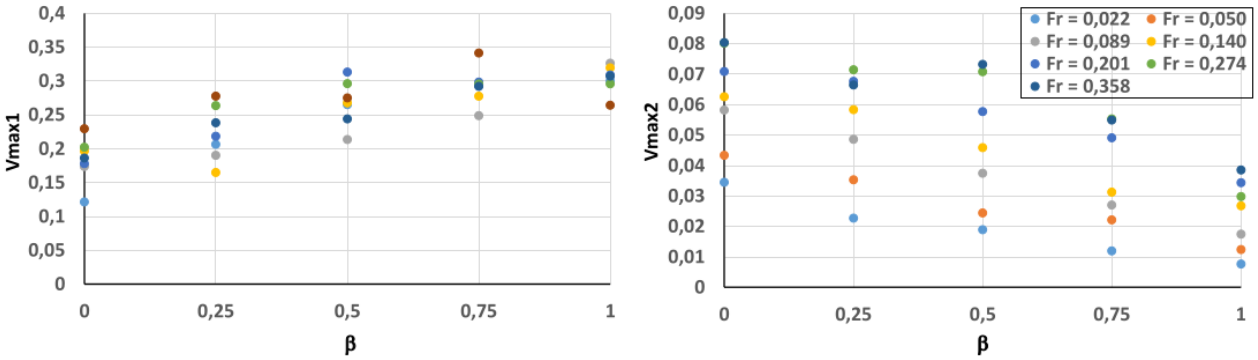


Fig. 8: Evolution of maximal velocity in zone I (left) and in zone II (right) as a function of height $\beta$

Evolutions of the maximal velocity in both zones are represented on Figure 8. Indeed, the decrease in zone I is to be associated with a higher obstruction of the flow by the pipe; hence more energy is dissipated in the flow to get past the pipe and less moving particles can overcome the pipe. The corresponding increase in zone II is associated to the fact that as initial height decreases, particle layers closer to the surface are coming into contact with the bottom of the pipe which have a higher velocity.

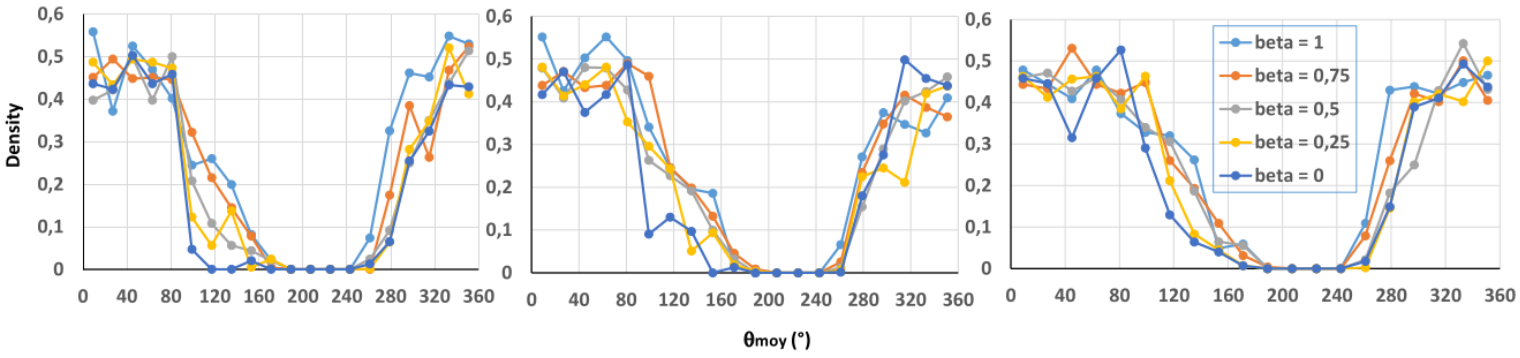


Fig. 9: Angular distribution of the packing fraction around the pipe for different initial heights $\beta$ at three different Froude number $Fr = 0.022$ (left); $Fr = 0.134$ (middle) ; $Fr = 0.274$ (right)

The width of zone III presents also an interesting feature with respect to the initial height (see Figure 9): the width of the depletion zone seems to increase

with a decreasing initial height as less incoming particles have sufficient energy to be able to get past the top of the pipe.

### *3.2.3. Influence of the relative size of the pipe*

Properties at contact are also very sensitive to the relative size of the pipe.

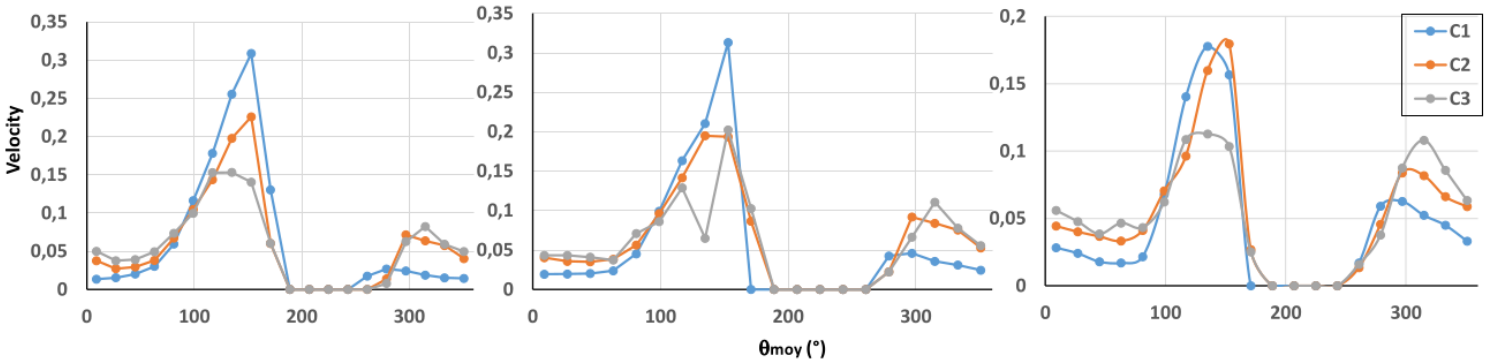


Fig. 10: Angular distribution of the velocity around the pipe for heights $\beta = 1$ (left) - $\beta = 0.5$ (middle) - $\beta = 0$ (right), a constant Froude number $Fr = 0.14$ and three different configurations of relative diameter ratio C1 ($R_d/R_p = 5$); C2 ($R_d/R_p = 10$); C3 ($R_d/R_p = 15$)

Figure 10 shows the typical velocity distribution for three different internal diameter ratio. As the relative diameter of the pipe increases, the velocities in zone I tend to increase as well as the velocities in zone II decrease. Decrease in zone II is consistent with the fact that deeper layers of the materials are involved in the flow downwards associated with lower velocity. Increase of velocity in zone I is also fairly consistent with different phenomena: First, considering particles with negligible velocity at the top of the pipe, the basic mechanical problem of a sphere rolling on a circular outline shows that the linear velocity of the rolling sphere in contact increases with the curvature radius because of the centrifugal force. Second, considering that the angle of take-off of the bead from the surface of the pipe is size independant, the distance of contact with the pipe is higher for higher diameters such that the drive from the particles of the superior layers at higher velocities applies on a longer distance. The evolution of the widths of the zone doesn't demonstrate specific correlations in the limit of the precisions of our computational procedure.

## 4. Conclusion

We proposed in this article a first contribution devoted to the characterisation of the flow of a granular material at the contact with a pipe in a rotating drum. This original device represents a new kind of mobile bed heat exchanger that may be potentially interesting for heat transfer intensification in different industrial processes as cooling, heating or heat recovery. As observed previously[18], the numerical approach can represent a reliable tool for novel design. We explored by the discrete element method the characteristics of the flow at the contact with the pipe as a function of the main control parameters of the problem (Froude number, Diameter ratio, relative height). We identified in particular a flow regime that we called *Biflow* where the flow of particles occurs at the top as well as the bottom of the pipe. This may be relevant for the transfer as it maximizes convection of particles at the boundary. We summarized all the phenomenology in a bed behavior diagram. In a second part, we precised the properties of the contact in the *Biflow* regime through the calculation of the packing fraction and the velocity field at the contact with the pipe. We observe in particular that the Froude number has an influence on the magnitude of the velocity only at the bottom of the pipe (low velocity zone) suggesting different mechanisms of transport on each side of the pipe. The initial height is a crucial factor in order to determine the magnitude of the velocities on the top side and the bottom side of the pipe and the properties of the *Biflow* regime: As the height increases the velocity on the top of the pipe increases and the velocity at the bottom decreases. The depletion zone is also larger for lower heights. Also, because of a size effect, the diameter of the pipe has a clear influence on velocities. The proper scaling of these hydrodynamical properties should require a more complete analysis of the complex granular flow heterogeneities in the entire drum which remains to be done beyond this first study. The trends obtained in this work may have clearly important consequences on the transfer in particular the width of the depletion zone. As noted previously, high velocities of the particles may favour transfer by allowing a more frequent renewal of particles at the boundary but the local density of particles has obviously a role to play in terms of transfer efficiency [11]. It is thus difficult to conclude at this stage because the zones of contact at a high velocity of particles (top of the pipe) are associated to lower values of density compared to the zones of contact at low velocity (bottom of the pipe) as observed on Figure 4. The relevance of the device for heat transfers has to be confirmed experimentally which is a purpose under way. Integration of heat transfers in the numerical model would also be a next stage in order to identify which dynamical regime may be optimal and to be able

to precise the correlation with the rheological properties of the granular material in this original device. The effect of the mixing properties of the granular material in the device after several rotations have also to be analysed as it may favour heat transfers [23]. The interplay between the convective transfer by particle mixing and the diffusive transfer through the contact network may be an important feature for the efficiency of the process.

**Acknowledgment**

We thank D. Flick for interesting discussions and L. Fournaison for a critical reading of the manuscript. This research was supported by an *ANS* grant from the National Research Institute for Agriculture, Food and the Environment (2022).

**References**

[1] Qoaider L.,Thabit Q., Kiwan S., (2017). Innovative sensible heat transfer medium for a moving bed heat exchanger in solar central receiver power plants. *Appl. Solar Energy, 53*,161–166

[2] Morris A.B., Ma Z., Pannala S., Hrenya C.M. (2016). Simulations of heat transfer to solid particles flowing through an array of heated tubes. *Solar Energy, 130*, 101-115

[3] Liu J., Yu Q., Peng J., Hu X., Duan W. (2015). Thermal Energy Recovery from High-Temperature Blast Furnace Slag Particles.*Int. Comm. in Heat and Mass Transfer, 69*, 23-28

[4] Guo Z., Tian X., Yang J., Shi T., Wang Q. (2021). Comparison of Heat Transfer in Gravity-Driven Granular Flow near Different Surfaces. *J. of Thermal Science, 30*, 441-450

[5] Andreotti B., Forterre Y., Pouliquen O. (2013). Granular media between fluid and solid. *Cambridge University Press*

[6] Rognon P., Einav I. (2010). Thermal Transients and Convective Particle Motion in Dense Granular Materials. *Phys.Rev.Lett., 105*, 218301

[7] Shauduri B., Muzzio F.J., Tomassone M.S. (2006). Modeling of heat transfer in granular flow in rotating vessels. *Chem. Eng. Sci., 61*, 6348-6360

[8] Shi D., Vargas W.L., McCarthy J.J.(2008). Heat transfer in rotary kilns with interstitial gases. *Chem. Eng. Sci., 63*, 4506-4516

[9] Emady H.N., Anderson K.V., Borghard W.G., Muzzio F.J., Glasser B.J., Cuitino A. (2016). Prediction of conductive heating time scales of particles in a rotary drum. *Chem. Eng. Sci. 152*, 45-54

[10] Adepu M., Chen S., Jiao Y., Gel A., Emady H. (2021). Wall to particle bed contact conduction heat transfer in a rotary drum using DEM. *Comp. Part. Mech., 8*, 589-599

[11] Morris A.B., Pannala S., Ma Z., Hrenya C.M. (2015). A conductive heat transfer model for particle flows over immersed surfaces. *Int. J. Heat and Mass Transfer, 89*, 1277-1289

[12] Teyar S., Renouf M., Berthier Y.(2019). Thermo-mechanical behavior of a granular media in a rotating drum. *Mechan. and Industry, 20(2)*, 203

[13] Tsotsas E. (2019). Particle-particle heat transfer in thermal DEM: Three competing models and a new equation. *Int. J. Heat and Mass Transfer, 132*, 939-943

[14] Herz F., Mitov I., Specht E., Stanev R. (2012). Experimental study of the contact heat transfer coefficient between the covered wall and solid bed in rotary drums. *Chem. Eng. Sci., 82*, 312-318

[15] Nafsun A.I., Herz F., Specht E., Scherer V., Wirtz S. (2016). Heat Transfer Experiments in a Rotary Drum for a Variety of Granular Materials. *Exp. Heat Transfer, 29*,1-16

[16] Adepu M., Boepple B., Fox B., Emady H. (2021). Experimental investigation of conduction heat transfer in a rotary drum using infrared thermography. *Chem. Eng. Sci., 230*, 116145

[17] Baumann T., Zunft S.. Development and performance assessment of a moving bed heat exchanger for solar central receiver power plants. *Energy Proc. 69*, 748-757

[18] Bartsch P., Zunft S. (2019). Granular flow around the horizontal tubes of a particle heat exchanger: DEM-simulation and experimental validation. *Solar Energy, 182*, 48-56

[19] Einav I., Rognon P., Miller T., Sulem J. (2018). Faults Get Colder Through Transient Granular Vortices. *Geophys. Res. Lett., 45*, 6

[20] Bongo Njeng A.S., Vitu S., Clausse M., Dirion J.L., Debacq M. (2018). Wall-to-solid heat transfer coefficient in flighted rotary kilns: experimental determination and modeling. *Exp. Thermal and Fluid Science,91*, 197-213

[21] Mellmann J. (2001). The transverse motion of solids in rotating cylinders—forms of motion and transition behavior. *Powder Technol., 118(3)*, 251-270

[22] Orozco L.F., Delenne J.Y., Sornay P., Radjai F. (2020). Rheology and scaling behavior of cascading granular flows in rotating drums. *J. of Rheology, 64*, 915

[23] Gui N., Yan J., Xu W., Ge L., Wu D., Ji Z., Gao J., Jiang S., Jang X. (2013). DEM simulation and analysis of particle mixing and heat conduction in a rotating drum. *Chem. Eng. Sci., 97*, 225-234

[24] Radjai F. and Dubois F. (2011). Discrete Numerical Modeling of Granular Materials. *Wiley-Iste ed.*

[25] Smilauer V. et al. (2021). *Yade Documentation 3rd ed. The Yade Project. DOI:10.5281/zenodo.5705394.* http://yade-dem.org

[26] Pournin L., Liebling T.M., Mocellin A. (2002). Molecular-dynamics force models for better control of energy dissipation in numerical simulations of dense granular media. *Phys. Rev. E, 65(1)*, 7

[27] J.-N. Roux, F. Chevoir (2011). Dimensional Analysis and Control Parameters, in Discrete-Element Modeling of Granular Materials, edited by F. Radjai, F. Dubois, (Wiley-Iste) pp. 199–232

[28] Aissa A.A., Duchesne C., Rodrigue D. (2012). Transverse mixing of polymer powders in a rotary cylinder part I: Active layer characterization. *Powder Technol., 219*, 193-201

## Appendix A.

You will find in the following a summary of the typology of the different flow patterns (velocity fields) in the parameter space (Fr, $\beta$, $R_d/R_p$)

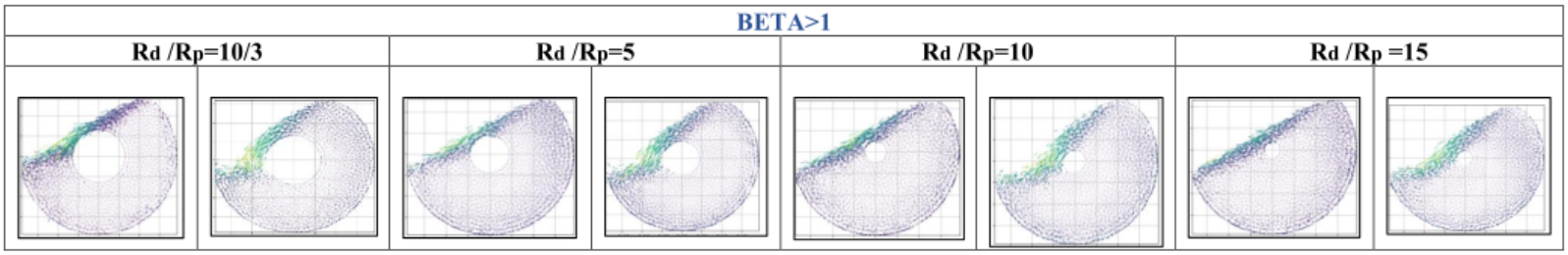


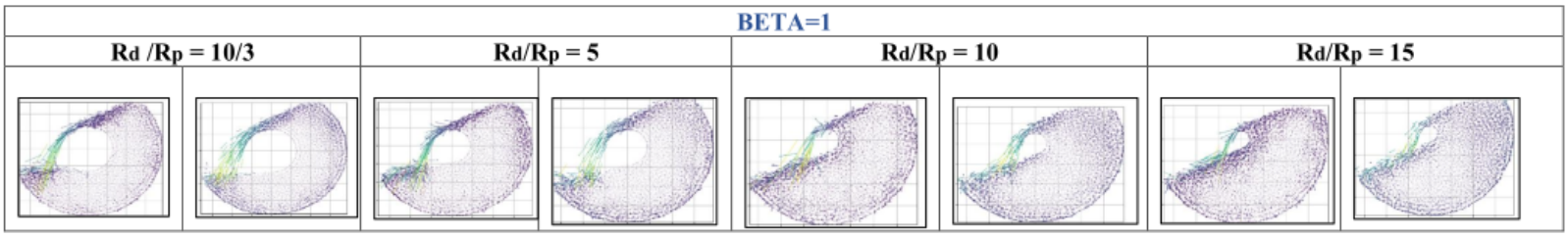


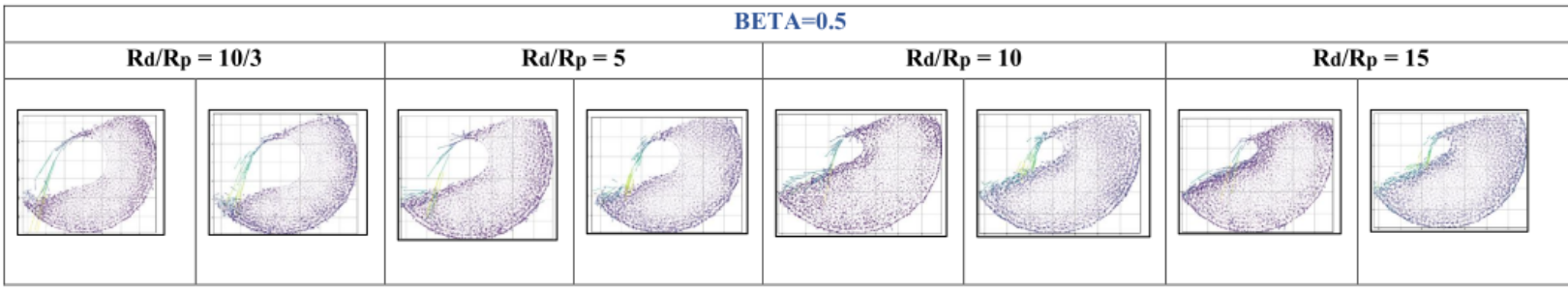

| BETA=0 | | | | | | | |
|---|---|---|---|---|---|---|---|
| **Rd/Rp = 10/3** | **Rd/Rp = 5** | | **Rd/Rp = 10** | | **Rd/Rp = 15** | |
| 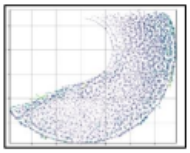 | 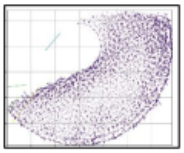 | 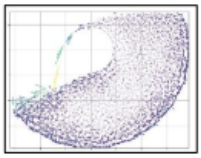 | 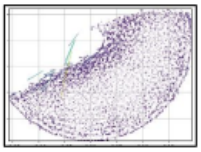 | 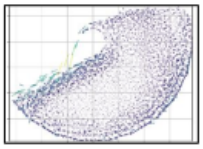 | 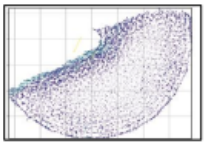 | 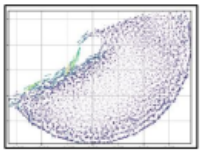 |

| BETA=-0.5 | | | |
|---|---|---|---|
| **Rd/Rp = 10/3** | **Rd/Rp = 5** | **Rd/Rp = 10** | **Rd/Rp = 15** |
| $2.24\times10^{-2}<Fr<3.57\times10^{-1}$ | $2.24\times10^{-2}<Fr<3.57\times10^{-1}$ | $2.24\times10^{-2}<Fr<3.57\times10^{-1}$ | $2.24\times10^{-2}<Fr<3.57\times10^{-1}$ |
| 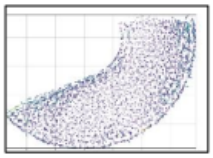 | 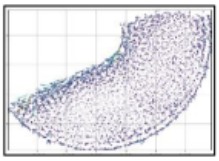 | 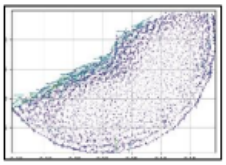 | 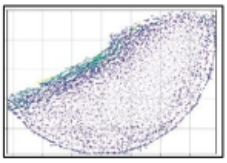 |

| BETA<-1 | | | |
|---|---|---|---|
| **Rd/Rp = 10/3** | **Rd/Rp = 5** | **Rd/Rp = 10** | **Rd/Rp = 15** |
| $2.24\times10^{-2}<Fr<3.57\times10^{-1}$ | | | |
| 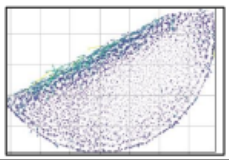 | | | |